MOX–Report No. 19/2009

A three-dimensional model for the dynamics and hydrodynamics of rowing boats

Luca Formaggia, Andrea Mola, Nicola Parolini and Matteo Pischiutta

MOX, Dipartimento di Matematica "F. Brioschi"
Politecnico di Milano, Via Bonardi 9 - 20133 Milano (Italy)

mox@mate.polimi.it http://mox.polimi.it

A three-dimensional model for the dynamics and hydrodynamics of rowing boats

Luca Formaggia, Andrea Mola, Nicola Parolini and Matteo Pischiutta

MOX - Modellistica e Calcolo Scientifico
Dipartimento di Matematica "F. Brioschi"
Politecnico di Milano
via Bonardi 9, 20133 Milano, Italy

Keywords: Computational Fluid Dynamics, Fluid structure interaction, Dynamics of rowing

AMS Subject Classification: 76T10, 74F10, 65M60

Abstract

This paper proposes a new model describing the dynamics of a rowing boat for general three dimensional motions. The complex interaction among the different components of the rowers/oars/boat system is analysed and reduced to a set of ordinary differential equations governing the rigid motion along the six degrees of freedom. To treat the unstable nature of the physical problem, a rather simple (but effective) control model is included, which mimics the main active control techniques adopted by the rowers during their action.

1 Introduction

Modelling a rowing boat is a challenging task due to the complexity of the rower/oars/hull system. Rowing boats are extremely narrow and light racing shells on which the rowers move on sliding seats, holding the handles of long oars, which are connected to the boat by means of oarlocks mounted on outriggers. With their back turned in the direction of the boat motion, the rowers produce the thrust needed to propel the boat forward by pulling the oar handles towards their chest: to make this operation more effective, the rowers start each *stroke* in a hunched position, and as they place the oar blades in the water, start pulling the oar handles towards them, sliding backwards on the seat, to exploit the power of the extending legs. When the legs are fully extended, and the hands have reached the chest, the *drive* phase terminates by removing the oars from the water, and the *recovery* phase, in which the rowers returns to the initial position, starts.

The simulation of the dynamics of a rowing scull is made difficult by the strong unsteadiness resulting from this complex kinematics of the rowers on board and by the interaction with the free surface of the fluid. Since the early works of F.H. Alexander [1], the topic of rowing boats dynamics in sculls has been widely investigated, although most of the technical

reports produced have been published only on the world wide web. Some of the most interesting contributions are those by W.C. Atkinson [2], A. Dudhia [6] and M. van Holst [24]. In [13] a rather complete mathematical model for boat dynamics is provided. However, all these models focus only on horizontal movements and use empirical formulas to simulate dissipative effects. The contribution of the vertical (heave) and lateral (sway) movement and angular rotations of the boat are indeed neglected. Several investigations have also been dedicated to the biomechanics of rowers movements, focusing on the correlation between forces and rower/oar kinematics [7] or analysing the different biomechanical factors that affect rowing performance (see [3] and references therein).

In [18] (see also [8]), a model for the symmetric dynamics of rowing boats has been introduced, accounting for the surge, heave and pitch motion. The model reconstructs the dynamics of the rower/oars/hull system, making use of experimental measurements for the imposition of the rowers kinematics and adopting a simplified hydrodynamic model accounting for the interaction with the water. The effect of shape, wave and viscous drag are computed using algebraic formulas, while hydrostatic forces, which depend on the wetted surface, are dynamically computed. The dissipative effects of waves generated by the secondary movements are dealt with by using a linear approximation of the water dynamics. Fluid-structure interaction procedures which include more complex fluid models (based on the Navier-Stokes equations) have been considered in [8].

In this paper, we extend the model proposed in [18] to arbitrary boat motions in the six degrees of freedom in order to be able to face a more general class of problem, including non-symmetric boat configurations.

The long length of a rowing boat and its semicircular cross-section makes it highly unstable, as any rower knows. The boat needs to be actively balanced by the rowers to avoid tipping. A mathematical description of this kind of human control and its implementation into the numerical model is not trivial. In this paper, we present a control model for roll and yaw accounting for the main action that the rowers employ to balance the boat. We will show through numerical examples the fundamental role that the control plays in simulations of three-dimensional dynamics of rowing boat.

A comparison between the results obtained using the reduced hydrodynamic model and the one based on the solution of the Navier-Stokes equations is also presented and discussed. This comparison highlights the weaknesses of the reduced model and helps formulating possible strategies to improve it.

2 A 6DOF dynamical model for rowing boats

In this section, we will introduce a mathematical model which describes the complex kinematics and dynamics of a rowing boat system and its interaction with the external environment.

The position and motion of each component on board (rowers, footboards, seats and oarlocks) are conveniently described with respect to a reference system fixed on the boat, while the boat dynamics is more easily described in an inertial frame of reference fixed on the race field.

The inertial reference system $(\mathbf{O}; X, Y, Z)$, which will be referred to as the *absolute coordinate system*, is fixed with the race field and we denote with $\mathbf{e}_X$, $\mathbf{e}_Y$ and $\mathbf{e}_Z$ the corresponding unit vectors. The X axis is horizontal, parallel to the undisturbed water free surface, and oriented along the direction of progression of the boat. The Z axis is vertical and pointing

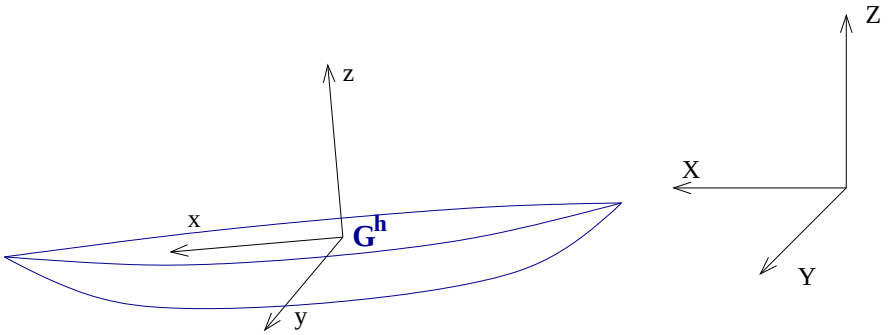

Figure 1: Rowing boat with relevant reference frames. The hull reference system is centered at hull center of mass.

upwards, while $\mathbf{e}_Y = \mathbf{e}_Z \times \mathbf{e}_X$. By convention, the origin $\mathbf{O}$ is at the start and the undisturbed water free surface is placed at the constant value $Z = h^0$.

A second reference system is attached to the boat and will be referred to as the *hull coordinate system*, $(\mathbf{G}^h; x, y, z)$), see Fig. 1. The unit vectors are $\mathbf{e}_x$, $\mathbf{e}_y$ and $\mathbf{e}_z$ are defined so that $\mathbf{e}_x$ and $\mathbf{e}_z$ identify the hull symmetry plane and $\mathbf{e}_z$ is directed from bottom to top, whereas $\mathbf{e}_x$ is from stern to bow. We point out that the hull reference system is centered in the hull center of mass $\mathbf{G}^h$ and not in the center of mass arising from hull and rowers system composition, the latter being not fixed due to the rowers motion.

Points in the absolute reference system will be indicated with uppercase letter, while the corresponding lowercase letter will indicate points in the hull reference frame. We can relate a point $\mathbf{P} = (P_X, P_Y, P_Z)$ in the absolute coordinate system and the corresponding point $\mathbf{p} = (p_x, p_y, p_z)$ in the hull coordinate system through the following relation

$$\mathbf{p} = \mathcal{R}(\psi, \theta, \phi) \left(\mathbf{P} - \mathbf{G}^h \right). \tag{1}$$

where $\mathcal{R}(\psi, \theta, \phi)$ denotes the rotation matrix

$$\mathcal{R}(\psi, \theta, \phi) = \begin{bmatrix} \cos\theta\cos\psi & \sin\phi\sin\theta\cos\psi - \cos\phi\sin\psi & \cos\phi\sin\theta\cos\psi + \sin\phi\sin\psi \\ \cos\theta\cos\psi & \sin\phi\sin\theta\sin\psi + \cos\phi\cos\psi & \cos\phi\sin\theta\sin\psi - \sin\phi\cos\psi \\ -\sin\theta & \sin\phi\cos\theta & \cos\phi\cos\theta \end{bmatrix}. \tag{2}$$

and the Euler angles ψ, θ and ϕ indicate the hull yaw, pitch and roll angles, respectively. With this conventions, a positive yaw occurs when the boat's bow displaces towards left; a positive pitch will instead determine a downwards movement of the bow; finally, with a positive roll angle, the left side of the boat will move upwards. The absolute velocity $\mathbf{V} = \dot{\mathbf{P}}$ of a generic point $\mathbf{P}$ and that relative to the hull system, $\mathbf{v}$, are related by

$$\mathbf{V} = \mathbf{v} + \dot{\mathbf{G}}^h + \dot{\mathcal{R}}^T \mathcal{R} \left(\mathbf{P} - \mathbf{G}^h \right) = \mathbf{v} + \dot{\mathbf{G}}^h + \boldsymbol{\omega} \times (\mathbf{P} - \mathbf{G}^h), \tag{3a}$$

where $\boldsymbol{\omega}$ is the angular velocity vector. As for the acceleration $\mathbf{A}$ of the generic point $\mathbf{P}$, the transformation between the local and the absolute reference reads

$$\mathbf{A} = \mathbf{a} + \ddot{\mathbf{G}}^h + \dot{\boldsymbol{\omega}} \times (\mathbf{P} - \mathbf{G}^h) + \boldsymbol{\omega} \times \boldsymbol{\omega} \times (\mathbf{P} - \mathbf{G}^h) + 2\boldsymbol{\omega} \times \mathbf{v}. \tag{3b}$$

The dynamics of the boat in the six degrees of freedom is described by the equations of linear and angular momentum, set in the inertial reference frame, and given by

$$
\begin{aligned}
M\ddot{\boldsymbol{G}}^c &= \sum_{j=1}^{n}(\boldsymbol{F}_{ol_j}+\boldsymbol{F}_{or_j})+\sum_{j=1}^{n}\boldsymbol{F}_{s_j} && \text{(4a)}\\
&+ \sum_{j=1}^{n}\boldsymbol{F}_{f_j}+M\boldsymbol{g}+\mathbf{F}^w \\
\mathcal{R}I_G\mathcal{R}^{-1}\dot{\boldsymbol{\omega}}+\boldsymbol{\omega}\times\mathcal{R}I_G\mathcal{R}^{-1}\boldsymbol{\omega} &= \sum_{j=1}^{n}\left[\left(\boldsymbol{X}_{ol_j}-\mathbf{G}^h\right)\times\boldsymbol{F}_{ol_j}+\left(\boldsymbol{X}_{or_j}-\mathbf{G}^h\right)\times\boldsymbol{F}_{or_j}\right] && \text{(4b)}\\
&+ \sum_{j=1}^{n}\left(\boldsymbol{X}_{s_j}-\mathbf{G}^h\right)\times\boldsymbol{F}_{s_j} \\
&+ \sum_{j=1}^{n}\left(\boldsymbol{X}_{f_j}-\mathbf{G}^h\right)\times\boldsymbol{F}_{f_j}+\mathbf{M}^w.
\end{aligned}
$$

where I_G is the hull tensor of inertia relative to the hull center of mass, expressed in the hull reference frame; $\boldsymbol{g}$ is the gravity acceleration and M is the mass of the hull. On the right hand side we have the external forces and momenta applied to the hull. They include the external forces exerted by the j-th rower on its left ($\boldsymbol{F}_{ol_j}$) and right oarlocks ($\boldsymbol{F}_{or_j}$), and on the seats ($\boldsymbol{F}_{s_j}$) and footboards ($\boldsymbol{F}_{f_j}$). The hydrodynamic interaction is given by the force $\mathbf{F}^w$ and the moment $\mathbf{M}^w$. In scull boats each rower uses two oars and non-zero values for both the left and right oarlock forces in (4) are assigned; on the other hand in sweep boats each rower uses only one oar and the oar forces on one side of each rowers has to be null.

Some of the forces exerted by a rower can be found from the equations governing the dynamics of the rowers. We represent the mass distribution of an athlete of given characteristics (weight, height, sex) by subdividing the body into $p = 12$ parts of which we infer the mass m_{ij} from anthropometric tables taken from [20]. Each part is then considered as concentrated in its own center of mass $\mathbf{X}_{ij}$, i.e. we neglect the angular inertia. The momentum equations for the j-th rower is then given by the following system

$$
\begin{aligned}
\sum_{i=1}^{p} m_{ij}\left(\ddot{\boldsymbol{X}}_{ij}-\boldsymbol{g}\right) &= \boldsymbol{F}_{hl_j}+\boldsymbol{F}_{hr_j} \;+\; \boldsymbol{F}_{sl_j}+\boldsymbol{F}_{sr_j}+\boldsymbol{F}_{fl_j}+\boldsymbol{F}_{fr_j} && \text{(5a)}\\
\sum_{i=1}^{p} m_{ij}\left(\boldsymbol{X}_{ij}-\mathbf{G}^h\right)\times\left(\ddot{\boldsymbol{X}}_{ij}-\boldsymbol{g}\right) &= \left(\boldsymbol{X}_{hl_j}-\mathbf{G}^h\right)\times\boldsymbol{F}_{hl_j}+\left(\boldsymbol{X}_{hr_j}-\mathbf{G}^h\right)\times\boldsymbol{F}_{hr_j} && \text{(5b)}\\
&+ \left(\boldsymbol{X}_{s_j}-\mathbf{G}^h\right)\times\boldsymbol{F}_{s_j}+\left(\boldsymbol{X}_{f_j}-\mathbf{G}^h\right)\times\boldsymbol{F}_{f_j}.
\end{aligned}
$$

Angular momentum is computed around the hull barycenter $\boldsymbol{G}^h$. $\boldsymbol{F}_{hl_j}$ and $\boldsymbol{F}_{hr_j}$ are the forces at the left and right hand of the j-th athlete, while $\boldsymbol{X}_{hl_j}$, $\boldsymbol{X}_{hr_j}$, $\boldsymbol{X}_{s_j}$, and $\boldsymbol{X}_{f_j}$ are the positions of the left and right hands, seats and foot-boards respectively.

The equations for the hull-rowers system are then obtained substituting into (4) the values of $\boldsymbol{F}_{s_i}+\boldsymbol{F}_{f_i}$ obtained from (5a) and the values of $\left(\boldsymbol{X}_{s_i}-\boldsymbol{G}^h\right)\times\boldsymbol{F}_{s_i}+\left(\boldsymbol{X}_{f_i}-\boldsymbol{G}^h\right)\times\boldsymbol{F}_{f_i}$ obtained from (5b), and read

$$
\begin{aligned}
M(\ddot{\mathbf{G}}^h - \boldsymbol{g}) &= \frac{r_h}{L}\sum_{j=1}^{n}(\boldsymbol{F}_{ol_j} + \boldsymbol{F}_{or_j}) && \text{(6a)}\\
&- \sum_{j=1}^{n}\sum_{i=1}^{p} m_{ij}\left(\ddot{\boldsymbol{X}}_{ij} - \boldsymbol{g}\right) + \mathbf{F}^w \\
\mathcal{R}I_G\mathcal{R}^{-1}\dot{\boldsymbol{\omega}} + \boldsymbol{\omega}\times\mathcal{R}I_G\mathcal{R}^{-1}\boldsymbol{\omega} &= \sum_{j=1}^{n}\left[\left(\boldsymbol{X}_{ol_j} - \mathbf{G}^h\right) - \frac{L-r_h}{L}\left(\boldsymbol{X}_{hl_j} - \mathbf{G}^h\right)\right]\times\boldsymbol{F}_{ol_j} \\
&+ \sum_{j=1}^{n}\left[\left(\boldsymbol{X}_{or_j} - \mathbf{G}^h\right) - \frac{L-r_h}{L}\left(\boldsymbol{X}_{hr_j} - \mathbf{G}^h\right)\right]\times\boldsymbol{F}_{or_j} \\
&- \sum_{j=1}^{n}\sum_{i=1}^{p}\left(\boldsymbol{X}_{ij} - \mathbf{G}^h\right)\times m_{ij}\left(\ddot{\boldsymbol{X}}_{ij} - \boldsymbol{g}\right) + \mathbf{M}^w. && \text{(6b)}
\end{aligned}
$$

Employing equations (3) to express rowers body parts positions and accelerations in the hull reference frame, we get the final system of ordinary differential equations for the unknowns $\mathbf{G}^h$ and $\boldsymbol{\omega}$

$$
\begin{aligned}
M_{Tot}\ddot{\mathbf{G}}^h + \dot{\boldsymbol{\omega}}\times\sum_{i,j} m_{ij}\mathcal{R}^T\boldsymbol{x}_{ij} &= \frac{r_h}{L}\sum_{j}(\boldsymbol{F}_{ol_j} + \boldsymbol{F}_{or_j}) - \sum_{i,j} m_{ij}\mathcal{R}^T\ddot{\boldsymbol{x}}_{ij} && \text{(7a)}\\
&- \sum_{i,j} m_{ij}\boldsymbol{\omega}\times\boldsymbol{\omega}\times\mathcal{R}^T\boldsymbol{x}_{ij} - \sum_{i,j} m_{ij}2\boldsymbol{\omega}\times\mathcal{R}^T\dot{\boldsymbol{x}}_{ij} + M_{Tot}\boldsymbol{g} + \mathbf{F}^w \\
\sum_{i,j} m_{ij}\mathcal{R}^T\boldsymbol{x}_{ij}\times\ddot{\mathbf{G}}^h + \mathcal{R}I_G\mathcal{R}^{-1}\dot{\boldsymbol{\omega}} &+ \sum_{i,j} m_{ij}\mathcal{R}^T\boldsymbol{x}_{ij}\times\dot{\boldsymbol{\omega}}\times\mathcal{R}^T\boldsymbol{x}_{ij} = -\boldsymbol{\omega}\times\mathcal{R}I_G\mathcal{R}^{-1}\boldsymbol{\omega} && \text{(7b)}\\
&- \sum_{i,j} m_{ij}\mathcal{R}^T\boldsymbol{x}_{ij}\times\mathcal{R}^T\ddot{\boldsymbol{x}}_{ij} - \sum_{i,j} m_{ij}\mathcal{R}^T\boldsymbol{x}_{ij}\times\boldsymbol{\omega}\times\boldsymbol{\omega}\times\mathcal{R}^T\boldsymbol{x}_{ij} \\
&- \sum_{i,j} m_{ij}\mathcal{R}^T\boldsymbol{x}_{ij}\times 2\boldsymbol{\omega}\times\mathcal{R}^T\dot{\boldsymbol{x}}_{ij} + \sum_{i,j}\mathcal{R}^T\boldsymbol{x}_{ij}\times m_{ij}\boldsymbol{g} + \mathbf{M}^w \\
&+ \sum_{j}\left[\left(\boldsymbol{X}_{ol_j} - \mathbf{G}^h\right) - \frac{L-r_h}{L}\left(\boldsymbol{X}_{hl_j} - \mathbf{G}^h\right)\right]\times\boldsymbol{F}_{ol_j} \\
&+ \sum_{j}\left[\left(\boldsymbol{X}_{or_j} - \mathbf{G}^h\right) - \frac{L-r_h}{L}\left(\boldsymbol{X}_{hr_j} - \mathbf{G}^h\right)\right]\times\boldsymbol{F}_{or_j}
\end{aligned}
$$

where $M_{Tot} = M + \sum_{i,j} m_{ij}$ indicates the total mass of the scull (encompassing both rowers and hull), and the indexes i and j in $\sum_{i,j}$ run from 1 to p and 1 to n, respectively. The first term in the right-hand-side of (7a) and the last two terms in (7b) include the blade contribution, where a simple lever model is used (see [19] for details). More sophisticated blade models accounting for the blade deformation and the local hydrodynamics are available in the literature [4, 5]; however, a detailed analysis of the blade contribution on the global rowing performance goes beyond the scope of this paper.

To close equations (7) we need to provide adequate models for the motion law of the rowers, oarlock forces and the fluid-dynamic forces and momenta $\mathbf{F}^w$ and $\mathbf{M}^w$. The rower kinematics has been reconstructed using image processing techniques on movies of athletes acting on a rower machine [10].

Each stroke period T is subdivided into an *active* phase with time length τ_a and a *recovery* phase with time length $\tau_r = T - \tau_a$. The duration of the active and recovery phases depends on the cadence (see [19]). We can formulate a simple model for the time evolution of the longitudinal and vertical oarlock forces over one stroke period based on the following relations

(well fitting the available measurements):

$$f_{o,x} = \begin{cases} F_x^{max} \sin(\frac{\pi t}{\tau_a}), & \text{if } 0 \le t \le \tau_a \\ 0 & \text{if } \tau_a < t \le T \end{cases}, \qquad f_{o,z} = \begin{cases} F_z^{max} \sin(\frac{\pi t}{\tau_a}), & \text{if } 0 \le t \le \tau_a \\ 0 & \text{if } \tau_a < t \le T \end{cases}, \tag{8}$$

where typical values of maximum forces are $F_x^{max} = 1200$ N and $F_z^{max} = 200$ N. In this model only the cadence and the maximum force is used to parametrize the time distribution of the oarloak force over a rowing period. When measurements for a specific athlete are available, these can be easily be included in the model to better characterize the rower force pattern. The contribution of the hydrodynamic forces and moments in (7) can be computed based on different models that will be recalled in Section 3.

2.1 Time advancing scheme for the boat dynamics

In order to express in a matrix form the cross products on the left hand side of system (7), we first define the following skew-symmetric matrices

$$A = -\sum_{i,j} m_{ij} \begin{bmatrix} 0 & -v_{ij}^3 & v_{ij}^2 \\ v_{ij}^3 & 0 & -v_{ij}^1 \\ -v_{ij}^2 & v_{ij}^1 & 0 \end{bmatrix}, \quad B = -\sum_{i,j} m_{ij} \begin{bmatrix} 0 & -v_{ij}^3 & v_{ij}^2 \\ v_{ij}^3 & 0 & -v_{ij}^1 \\ -v_{ij}^2 & v_{ij}^1 & 0 \end{bmatrix}^2$$

where

$$\boldsymbol{v}_{ij} = \{v_{ij}^1, v_{ij}^2, v_{ij}^3\} = \mathcal{R}^T \boldsymbol{x}_{ij}.$$

We can now write

$$\mathcal{M}(t) = \begin{bmatrix} M_{Tot} I & A \\ -A & \mathcal{R} I_G \mathcal{R}^{-1} + B \end{bmatrix}$$

where I is the identity matrix of order 3. The right hand side of system (7) can then be written in the vector form $\boldsymbol{f} = \boldsymbol{f}^i + \boldsymbol{f}^w$, where

$$\boldsymbol{f}^i(\dot{\mathbf{G}}^h, \mathbf{G}^h, \boldsymbol{\omega}) = \begin{Bmatrix} \frac{r_h}{L} \sum_j \boldsymbol{F}_{o_j} - \sum_{i,j} m_{ij} \mathcal{R}^T \ddot{\boldsymbol{x}}_{ij} - \sum_{i,j} m_{ij} \boldsymbol{\omega} \times \boldsymbol{\omega} \times \mathcal{R}^T \boldsymbol{x}_{ij} \\ - \sum_{i,j} m_{ij} 2\boldsymbol{\omega} \times \mathcal{R}^T \dot{\boldsymbol{x}}_{ij} + M_{Tot} \boldsymbol{g} \\ \\ -\boldsymbol{\omega} \times \mathcal{R} I_G \mathcal{R}^{-1} \boldsymbol{\omega} - \sum_{i,j} m_{ij} \mathcal{R}^T \boldsymbol{x}_{ij} \times \mathcal{R}^T \ddot{\boldsymbol{x}}_{ij} \\ - \sum_{i,j} m_{ij} \mathcal{R}^T \boldsymbol{x}_{ij} \times \boldsymbol{\omega} \times \boldsymbol{\omega} \mathcal{R}^T \boldsymbol{x}_{ij} \\ - \sum_{i,j} m_{ij} \mathcal{R}^T \boldsymbol{x}_{ij} \times 2\boldsymbol{\omega} \times \mathcal{R}^T \dot{\boldsymbol{x}}_{ij} + \sum_{i,j} \mathcal{R}^T \boldsymbol{x}_{ij} \times m_{ij} \boldsymbol{g} \\ + \sum_j \left[\left(\boldsymbol{X}_{o_j} - \mathbf{G}^h \right) - \frac{L - r_h}{L} \left(\boldsymbol{X}_{h_j} - \mathbf{G}^h \right) \right] \times \boldsymbol{F}_{o_j} \end{Bmatrix}. \tag{9}$$

and

$$\boldsymbol{f}^w = \begin{Bmatrix} \mathbf{F}^w \\ \mathbf{M}^w \end{Bmatrix}$$

In this way, once defined the variable $\boldsymbol{u} = \begin{Bmatrix} \dot{\mathbf{G}}^h \\ \boldsymbol{\omega} \end{Bmatrix}$, system (7) can be recast in the following form

$$\mathcal{M}(t) \dot{\boldsymbol{u}} = \boldsymbol{f}(\boldsymbol{u}, t).$$

The resulting system can be further modified to obtain a first order non-linear ODE system, more suitable for the numerical solution. Defining

$$M(t) = \begin{bmatrix} [I] & 0 \\ 0 & [\mathcal{M}(t)] \end{bmatrix}, \qquad \boldsymbol{y} = \begin{Bmatrix} \mathbf{G}^h \\ \boldsymbol{u} \end{Bmatrix}, \qquad \boldsymbol{F}(\boldsymbol{y}, t) = \begin{Bmatrix} \dot{\mathbf{G}}^h \\ \boldsymbol{f} \end{Bmatrix}$$

we can finally write the system

$$\dot{\boldsymbol{y}} = (M(t))^{-1}\, \boldsymbol{F}(\boldsymbol{y}, t), \tag{10}$$

which is solved by means of a Runge–Kutta–Fehlberg 45 time advancing scheme available in the Gnu Scientific Library [9].

For each time step, it will be necessary to compute the rotation matrix $\mathcal{R}$ appearing in the motion equations. To do this, equation (2) is employed, once the unit vectors describing the orientation of the hull at the new time step $n+1$ are obtained by means of the trapezoidal rule, namely

$$\begin{aligned}
\boldsymbol{e}_{x_{n+1}} &= \boldsymbol{e}_{x_n} + \frac{\Delta t}{2}(\omega_{n+1} + \omega_n) \times \boldsymbol{e}_{x_n} \\
\boldsymbol{e}_{y_{n+1}} &= \boldsymbol{e}_{y_n} + \frac{\Delta t}{2}(\omega_{n+1} + \omega_n) \times \boldsymbol{e}_{y_n} \\
\boldsymbol{e}_{z_{n+1}} &= \boldsymbol{e}_{x_{n+1}} \times \boldsymbol{e}_{y_{n+1}}.
\end{aligned}$$

3 Hydrodynamic models

In the previous section, we have introduced the complex dynamical system which describes the motion of a rowing boat. The hydrodynamic forces and moments in (7) accounting for the interaction between the boat and the surrounding water should also be modelled. Different modelling choices are possible characterized by different level of accuracy and modeling (and computational) complexity. Simplified models based on algebraic relations and potential flow theory can be adopted for a preliminary design or to compare different rowing techniques, as they are very efficient computationally and can provide solutions in few minutes. More advanced model based on the solution of the Navier-Stokes equations can also be coupled to the dynamical system in order to obtain more reliable flow fields and force estimates. However, in this case, the computational cost rises up to several hours for each simulations. Hereafter, we briefly describe these two approaches that have been used in our simulations. A third approach of intermediate complexity, based on nonlinear potential theory and boundary element discretization, is currently being developed [19].

3.1 Reduced algebraic/potential model

A reduced model for the computation of the hydrodynamic action on the boat has been developed in the past years [18] which can be used for fast evaluation of the fluid-structure interaction during a rowing race.

The model is based on the assumption that the boat motion can be decomposed into a main motion (constant velocity in the course direction) and secondary motions in all the six degrees of freedom.

The forces and angular moments associated to the mean motion are obtained based on algebraic formulae. The different component of the drag (shape, viscous and wave resistance) as well as lift and pitching moment are computed based on the boat velocity, force and moment coefficients and the hydrostatic contribution given by the actual attitude of the boat. The forces and moment coefficients are obtained from standard ITTC correlations [11] and classical Michell's integrals [16] or based on complete CFD simulation performed off-line on a steady boat configuration.

The forces and moments associated to the secondary motions are obtained as the action of the radiation of the gravity waves generated by the secondary motion. These can be computed resorting to the solution of a linearized potential problem for the flow generated by a boat oscillating in the different degrees of freedom. The methodology has been introduced in [15] (see also [18]) and is used to compute an added mass matrix and a damping matrix which enter as additional contributions into system (10).

3.2 Full Navier-Stokes model

A more reliable (and more expensive) alternative for the evaluation of the hydrodynamic action has been developed based on the solution of the incompressible Reynolds-Averaged Navier–Stokes (RANS) equations . The discrete solution of the Navier–Stokes equations is achieved using a SIMPLE method [22] for the pressure-velocity decoupling, finite volume discretization in space and a semi-implicit time integration. In order to solve a turbulent free-surface flows, the Navier–Stokes equations are coupled with a transport equation for the phase volume fraction (using the so-called Volume of Fluid (VOF) method) and with a standard $k - \varepsilon$ two equation model for turbulence. The fluid-structure coupling algorithm is based on a staggered approach where the flow is computed for a given boat position; then, based on the velocity and pressure distributions, the hydrodynamic force and moment acting on the boat are computed and passed to the dynamical system (10) which is advanced in time. The updated values of linear and angular velocity are then passed back to the flow solver and used to deform the computational grid for the solution of the flow at the new time step. For details on the flow solver and the fluid-structure interaction we refer to [21, 23, 8].

4 A model for the active rowers control

The three-dimensional rowing boat dynamics model just introduced is inherently unstable. If we consider the free body diagram for the roll degree of freedom presented in Fig. 2, we notice that for these boats the hydrostatic buoyancy force is applied in a pressure center which is lower than the global center of gravity. The resulting roll moment grows with the roll angle, and makes the system unstable on this degree of freedom. Moreover, possible non-symmetric oarlock forces (typical of sweep boats) might increase the instability of the system.

Furthermore, due to the lack of a yaw component of the hydrostatic force, the equilibrium about this degree of freedom is indifferent (see Fig. 3). Thus, if non-symmetric forces are applied at the oarlocks, the resulting torque will not be counteracted by any restoring term, and the boat will rotate. Of course, the viscous effects are too small to be able to damp this movement.

During their rowing action, the athletes constantly apply an active control to the boat, in order to stabilize the boat roll, and keep the boat moving straight towards the finish line. In the following sections, we will illustrate how such control has been modeled and implemented in the rowing boat model.

4.1 Roll control

As illustrated in Fig. 2, we assume that the rowers keep the boat in the equilibrium position by exerting opposite vertical forces on the left and right oarlock. In this way, whenever the boat is not perfectly vertical, they produce a restoring moment which stabilizes the system. We

have modelled the controlling action of the rowers on the roll movement with a restoring force proportional to the roll angle defining an additional contribution on the vertical component in (8), namely

$$\Delta F_{o,z} = \pm k_{\text{Roll}}\phi,$$

where k_{Roll} is the gain coefficient. With the assumed conventions, for positive roll angle, $\Delta F_{o,z}$ is positive (resp. negative) on the left (resp. right) oarlock. The oarlock forces needed to keep the boat vertical are very small, and the rowers obtain them by moving the oars handles slightly. Thus, this control is acting also during the recovery phase of the stroke, when the oars are not in the water.

4.2 Yaw control

A first device to control the boat on the yaw degree of freedom is a fin placed towards the stern of the hull. This small appendage is usually a flat plate characterized by a surface area S_f and an aspect ratio λ_f. The drag and lift coefficients of the fin have been obtained based on the following relations, valid for wings of finite span [12]

$$C_{Lf} = 2\pi \frac{|\alpha_f|}{1 + 1/(\lambda_f)}, \qquad C_{Df} = \frac{{C_{Lf}}^2}{2\lambda_f},$$

where the fin angle of attack α_f is given by

$$\alpha_f = -\psi + \arcsin\left(\frac{\dot{G}^h_y - \omega_x d_z + \omega_z d_x}{|\dot{\mathbf{G}}^h|}\right),$$

d_x and d_z being respectively the longitudinal and vertical distances between the fin pressure center and the hull center of gravity.

The fin force in the relative reference frame is finally

$$\boldsymbol{f}_f = \frac{1}{2}\rho_w |\dot{\mathbf{G}}^h|^2 S_f \left\{ \begin{array}{c} (-C_{Df}\cos\alpha_f + C_{Lf}|\sin\alpha_f|) \\ \frac{\alpha_f}{|\alpha_f|}\left(C_{Lf}\cos\alpha_f + C_{Df}|\sin\alpha_f|\right) \\ 0 \end{array} \right\}$$

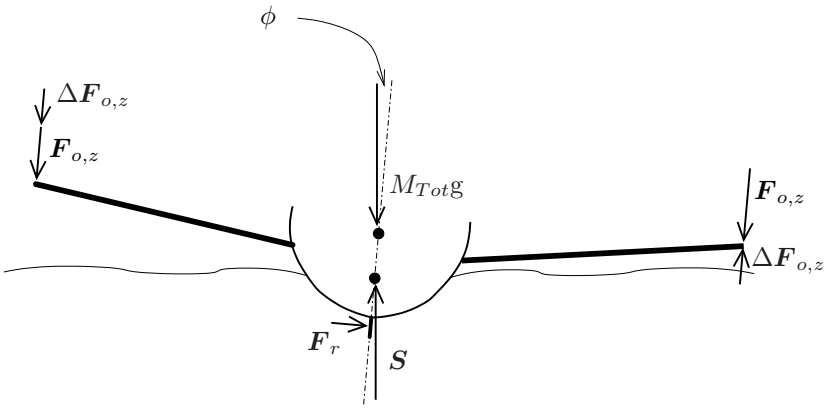

Figure 2: A front view of the boat with the vertical forces applied to the hull.

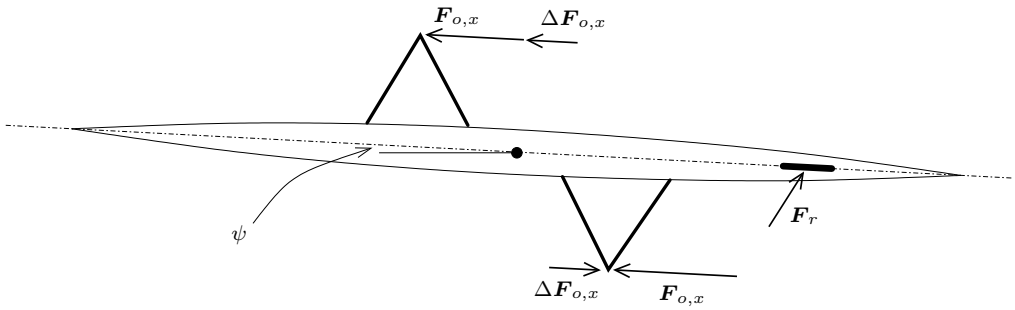

Figure 3: A top view of the boat with the longitudinal forces applied to the hull.

The fin acts as a (nonlinear) damper for the yaw motion. Nevertheless, it does not provide a restoring force able to keep the boat moving straight towards the finish line. During a race, such restoring force is provided by the rowers, who modulate their oar forces on the right and left side of the boat in order to prevent it from progressively turn sideways.

In our model, the yaw control is only operating during the active phase of the stroke. At the beginning of each stroke, the rower evaluates the instantaneous yaw angle ψ_0 and modulates the longitudinal maximum force of the stroke through an additional component on the longitudinal component in (8), namely

$$f_{o,x} = \begin{cases} (F_x^{max} \pm k_{\text{Yaw}}\psi_0)\sin(\frac{\pi t}{\tau_a}), & \text{if } 0 \le t \le \tau_a \\ 0 & \text{if } \tau_a < t \le T \end{cases},$$

k_{Yaw} being the gain coefficient of the yaw control. With the assumed conventions, for positive yaw angle, the additional term $\Delta F_{o,x} = \pm k_{\text{Yaw}}\psi_0$ is positive (resp. negative) on the right (resp. left) oarlock.

The assumption that the rowers decide at the beginning of each stroke how to control the boat yaw is based on the fact that for the rowers it is very difficult to modulate the strength of the stroke during the active phase, as the latter is usually a short and intense pulling motion. On the other hand, they can exploit the recovery phase to decide how to adjust the strength of the next stroke in order to keep the boat moving in the correct direction. Finally, we would like to emphasize that although the control model proposed is rather simple, it allowed us to simulate the six degrees of freedom problem, which is physically unstable, thus broadening the range of rowing boat classes that can be simulated by our model. Further improvements of this control model can be envisaged for the future and should include, for instance, the contribution of the active rudder used by the coxswain for boat steering.

5 Numerical results

The model presented in this paper has been adopted to simulate the dynamics of rowing boats in the framework of the partnership between our research group and Filippi Lido s.r.l., a world leader rowing boat manufacturer. Results for symmetric dynamics (with only surge, heave and pitch degrees of freedom activated) obtained with the reduced hydrodynamic model have been presented in [18, 8]. In this section we describe an example of simulation obtained with the reduced model on a 6DOF dynamics highlighting the role of the control. Finally, an example of fluid-structure interaction based on the Navier–Stokes hydrodynamic model is presented and discussed.

5.1 Dynamics of a rowing boat in 6DOF

The idea underlying the effort of developing a complete three-dimensional model for rowing dynamics was to extend the range of application of the model, enabling the possibility to analyse non-symmetric configurations. Hereafter, we present a test case that has been designed in order to investigate the behavior of the model for non-symmetric problems. We consider a men's coxless four rowing race with a non-symmetric distribution of the oarlock forces. In particular, each rower exerts on the oarlock longitudinal and vertical forces with maximum amplitude of $F_x^{max} = 1200$ N and $F_z^{max} = 200$ N, respectively. For only the bowman we consider different values of forces, $F_x^{max} = 1300$ N and $F_x^{max} = 230$ N, respectively. In these simulations, we have considered boat and rower weight of 49.6 kg and 85 kg, respectively. The rowing cadence is 40/min which results in an active phase duration of 0.712 s. The rowing angle of catch and finish are 65 and 45 degrees, respectively. The non-symmetric distribution of oarlock forces generates a full dynamics in the six degrees of freedom, as presented in Fig. 4. As a result of the control described in Section 4 the time evolution of the yaw angle reaches an asymptotic behavior oscillating around an equilibrium angle. The roll angle also oscillates around a small asymptotic mean value. This different behavior can be correlated to the different control system (continuous for roll and discrete for yaw) for the two degrees of freedom. The sway degree of freedom is not controlled and we noticed that the boat presents a monotonic sway which, however, can be consider negligible for the performance estimation.

To better appreciate the fundamental role that an active control has when considering dynamics on the six degrees of freedom, we compare the results obtained with and without the control contribution. The roll and yaw instabilities that arise when no control is adopted are displayed in Fig. 5 and confirm the absolute need of a control procedure. The trajectory on the water plane is presented in Fig. 6 showing the divergence of the sway degree of freedom when the control is absent.

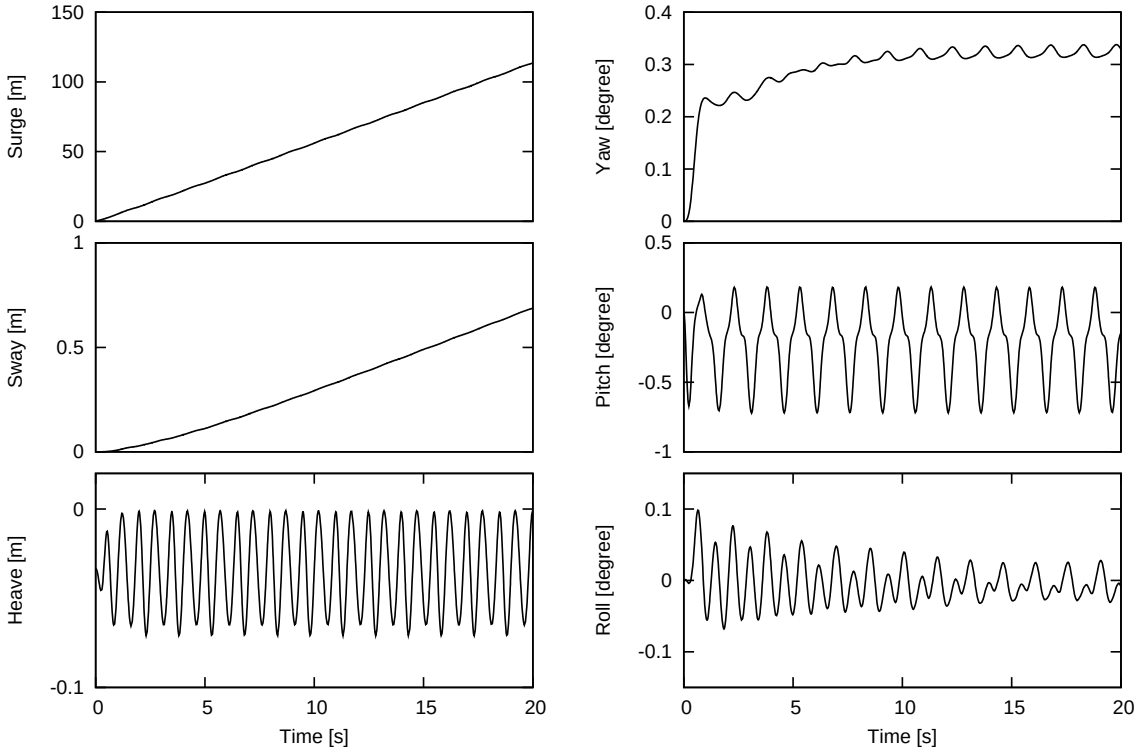

Figure 4: Time evolution of the six degrees of freedom for a non-symmetric men's coxless four boat configuration.

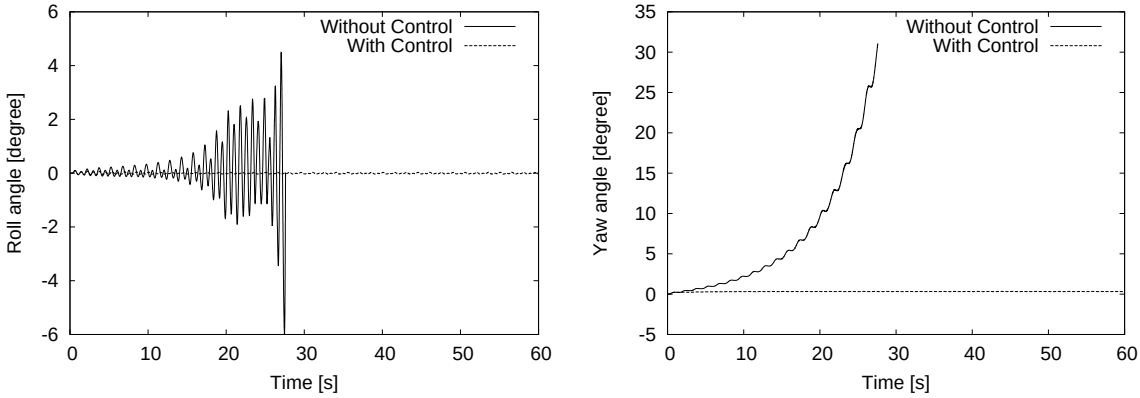

Figure 5: Time evolution of roll (left) and yaw (right) angles during the first 60 seconds of the race simulation with and without the control.

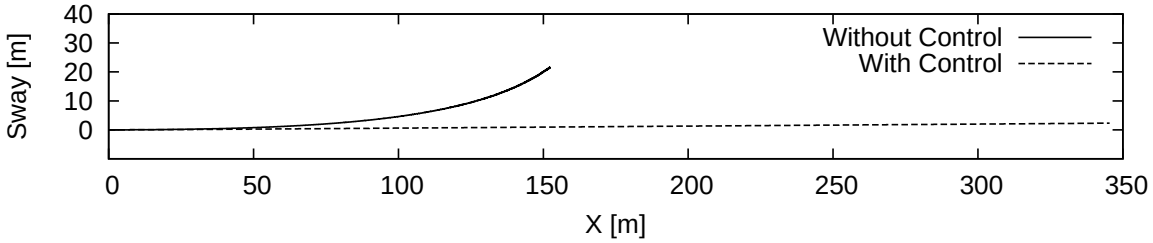

Figure 6: Boat trajectory during the first 60 seconds of the race simulation with and without the control (equal scale in x and y axes).

5.2 FSI with the Navier–Stokes model

In this section we present the results of simulations carried out using the Navier-Stokes equations to estimate the interaction of the boat with the free-surface flow. Here we consider a symmetric men's quadruple scull with only surge, heave and pitch as active degrees of freedom. The simulation is initialized by the steady solution obtained on a fixed boat configuration moving at 5.3 m/s. We have considered two different computational grids with 220,000 and 550,000 elements, respectively. In these simulations, we have considered on each oarlock longitudinal and vertical forces with maximum amplitude of $F_x^{max} = 625$ N and $F_z^{max} = 104$ N, respectively. Boat and rower weight are 52 kg and 90 kg, respectively. The rowing cadence is 39.5/min which results in an active phase duration of 0.71 s.

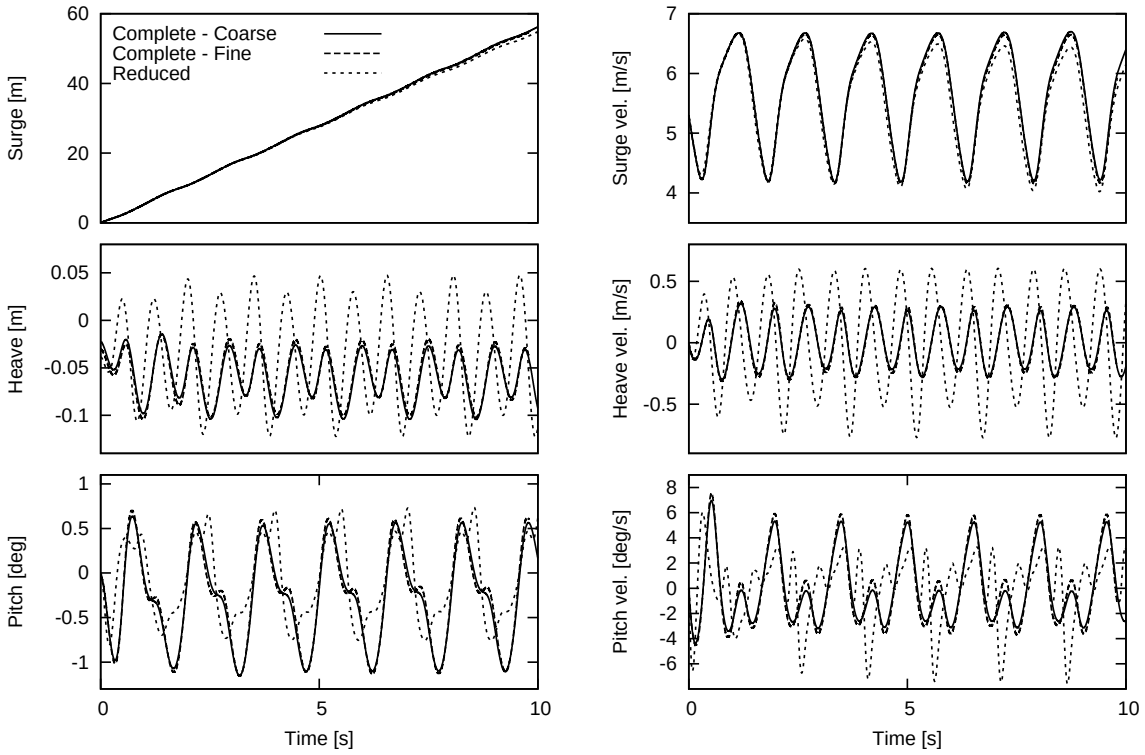

Figure 7: Boat dynamics obtained with the Navier–Stokes model for the two grids and with the reduced hydrodynamic model. From top to bottom: horizontal position and sink of the center of mass and pitching angle (left) and correspondent velocities (right).

The results of the simulations on the two computational grids are reported in Fig. 7 and compared with the result obtained with the reduced hydrodynamic model. The time evolution of the different degrees of freedom obtained with the two grid resolutions are globally very close. We can notice a slightly higher mean value of the heave oscillation and a larger amplitude of the pitch dynamics for the fine grid. The comparison with the reduced model shows that the kinematics along the longitudinal direction (which is the fundamental performance indicator) is reasonably well captured. However, large discrepancy can be observed for the heave degree of freedom, where the amplitude of the oscillation is largely overestimated by the reduced

model.

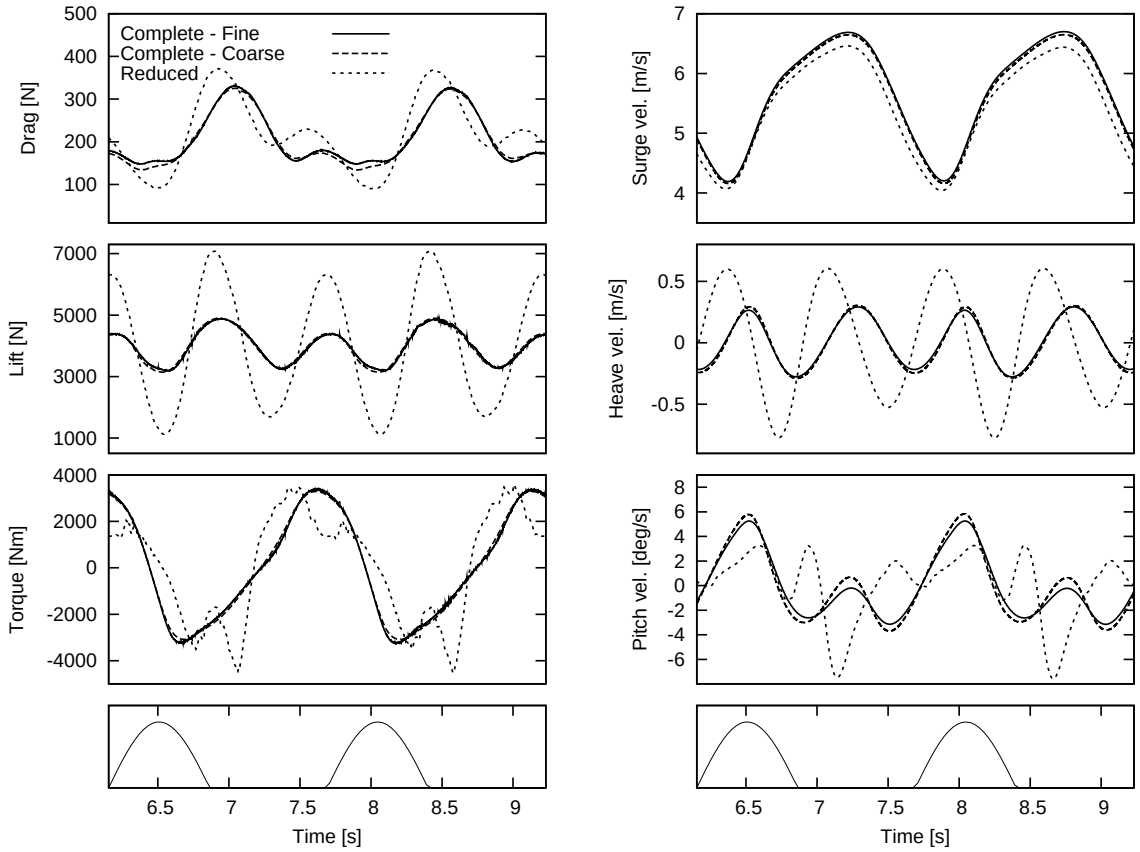

Figure 8: Drag, lift and pitching moment (left) and correspondent velocities (right) for the complete and reduced models over two stroke periods; active phase of the stroke is shown as reference in bottom row.

In Fig. 8 we report the time evolution of forces and moments (and the correspondent velocities) over two rowing periods obtained with the full and reduced hydrodynamic models. The active phase of the stroke is also shown as reference over the period. We can notice how the main discrepancy on the heave dynamics is due to an overprediction of the lift oscillation amplitude which can be correlated to a poor estimation of the damping matrix coefficient associated to this degree of freedom. A possible strategy to improve the behavior of the reduced model is to use a finer grid for the numerical solution of the potential flow problem adopted to estimate the effect on the boat dynamics of the gravitational waves generated by the secondary motion. Analyses in this direction are currently under investigation. The estimate for the pitching moment looks reasonably accurate in the reduced model; however, frequencies higher that the main rowing frequency appear in the time signal for the reduced model, thus downgrading the predicted dynamics for pitching. This is due to the fact that the reduced model the damping matrix is here computed based on one single frequency. We are confident that the ongoing development (see [19]) of a strategy for the damping matrix evaluation based on the convolution integral over a range of frequency [14] will cure this problem.

6 Conclusions

A complete dynamical model for rowing boats has been presented in this work. Such model is parametrized in function of the athlete and boat characteristics and can be employed for boat design, performance prediction and as support for training. In particular, the model predicts the boat motion in all its six degrees of freedom, so that both scull and sweep boats can be considered. The dynamical model has been coupled with two hydrodynamic models characterized by different levels of modelling and computational complexity. Numerical results obtained with the different schemes have been presented and compared in order to highlight the correspondent advantages and weaknesses. Possible further developments for the reduced model have also been discussed which could improve its behavior on performance prediction. At the time being, a validation study is under way using measurements taken from a rowing boat equipped with accelerometers and ergometers. The results are rather encouraging, yet too preliminary to be included in this work, which focuses most on the mathematical modelling side. It will be the subject of a forthcoming paper.

References

[1] F. H. Alexander. The theory of rowing. In G. W. Todd, editor, *Proceedings of the University of Durham Philosophical Society*, volume VI, Newcastle-upon-Tyne, England, 1925. Andrew Reid & Co.

[2] W.C. Atkinson. Modeling the dynamics of rowing. www.atkinsopht.com, 2002.

[3] A. Baudouin, D. Hawkins. A biomechanical review of factors affecting rowing performance. Br. J. Sport Med. 2002;35:396-402.

[4] N. Caplan, T. Gardner. A mathematical model of the oar blade-water interaction in rowing. J. Sport Science 2007;25(9):1025-1034.

[5] A. Coppel, T. Gardner, N. Caplan, D. Hargreaves. Numerical Modelling of the Flow Around Rowing Oar Blades. The Engineering of Sport 2008;7(1):353-361.

[6] A. Dudhia. The physics of rowing. www.atm.ox.ac.uk/rowing/physics, 2001.

[7] B. Elliott, A. Lyttle, O. Birkett. The RowPerfect Ergometer: a training aid for on-water single scull rowing. Sport Biomech. 2002;1(2):123-134.

[8] L. Formaggia, E. Miglio, A. Mola, and N. Parolini. Fluid-structure interaction problems in free surface flows: application to boat dynamics. Int. J. Num. Meth. Fluids 2008; 56(8):965-978

[9] M. Galassi, J. Davies, J. Theiler, B. Gough, G. Jungman, M. Booth, and F. Rossi. *GNU scientific library reference manual*. Network Theory Ltd, second edition, 2004.

[10] G. P. Grassi, T. Santini, N. Lovecchio, M. Turci, V.F. Ferrario and C. Sforza. Spatiotemporal consistency of trajectories in gymnastics: a three-dimensional analysis of flic-flac, *Int. J. Sports Med.* 2005; 26(2):134-8.

[11] J.B. Hadler. Coefficients for international towing tank conference 1957 model-ship correlation line. Technical Report 1185, David Taylor Model Basin, April 1958.

[12] K. Karamcheti. Principles of ideal fluid aerodynamics. *Wiley*, New York (USA), 1966.

[13] L. Lazauskas. A performance prediction model for rowing races. Technical Report L9702, Dept. of Appl. Math., University of Adelaide, Australia, 1997.

[14] S.-K. Lee. The calculation of zig-zag maneuver in regular waves with use of the impulse response functions. *Ocean Engineering* 2000, 27:87–96.

[15] C.C. Mei. *The applied dynamics of ocean surface waves.* World Scientific Publishing, Singapore, 1989. Second printing with corrections.

[16] J. H. Michell. The wave resistance of a ship. *Phil. Mag.* 1898; 45:106–123.

[17] A. Millward. A study of the forces exerted by an oarsman and the effect on boat speed. *J. Sports Sciences* 1987; 5:93–103.

[18] A. Mola, L Formaggia, and E. Miglio. Simulation of the dynamics of an olympic rowing boat. In *Proceedings of ECCOMAS CFD 2006,Egmond aan Zee, September 5-8, The Netherlands.* TU Delft, 2006. ISBN: 90-9020970-0.

[19] A. Mola. Models for Olympic rowing boats. *PhD Thesis*, Politecnico di Milano, 2009.

[20] *Man-System Interaction Standards – Volume 1.* NASA Technical Standards, 1995.

[21] N. Parolini and A. Quarteroni. Modelling and numerical simulation for yacht design. In *Proceedings of the 26th Symposium on Naval Hydrodynamics* Strategic Analysis, Inc., Arlington, VA, USA, 2007.

[22] S. V. Patankar. Numerical heat transfer and fluid flow. Hemisphere Publishing Corp., Washington, DC, USA, 1980.

[23] M. Pischiutta. Dinamica di una imbarcazione da canottaggio: simulazioni numeriche con un modello RANS. Master Thesis, Politecnico di Milano, 2008.

[24] M. van Holst. On rowing. http://home.hccnet.nl/m.holst/RoeiWeb.html, 2004.

MOX Technical Reports, last issues

Dipartimento di Matematica "F. Brioschi",
Politecnico di Milano, Via Bonardi 9 - 20133 Milano (Italy)

19/2009 L. Formaggia, A.Mola, N. Parolini, M. Pischiutta:
A three-dimensional model for the dynamics and hydrodynamics of rowing boats

18/2009 J. Silva Soares, P. Zunino:
A mathematical model for water uptake, degradation, erosion, and drug release from degradable polydisperse polymeric networks

17/2009 M. Longoni, C. Magistroni, P. Ruffo, G. Scrofani:
3D Inverse and Direct Structural Modeling Workflow

16/2009 G. Aletti, C. May, P. Secchi:
A functional equation whose unknown is P([0; 1]) valued

15/2009 S. Perotto, A. Ern, A. Veneziani:
Hierarchical local model reduction for elliptic problems I: a domain decomposition approach

14/2009 L. Beirão da Veiga, M. Verani:
A posteriori boundary control for FEM approximation of elliptic eigenvalue problems

13/2009 E.Miglio, A. Villa:
A mathematical derivation of compaction and basin models

12/2009 S. Badia, A. Quaini, A. Quarteroni:
Coupling Biot and Navier-Stokes equations for modelling fluid-poroelastic media interaction

11/2009 L. Formaggia, A. Villa:
Implicit tracking for multi-fluid simulations

10/2009 P. Zunino:
Numerical approximation of incompressible flows with net flux defective boundary conditions by means of penalty techniques